MINI REVIEWS

Short reviews with lasting impact

Mini Reviews in *CCS Chemistry* are short and comprehensive overviews of a specific research topic that provide an introduction to research covering all areas of chemistry and the chemical sciences. With over 100 open access Mini Reviews in the journal, readers can freely explore and learn about a variety of topics. All of our Mini Reviews can be viewed at:
https://www.chinesechemsoc.org/journal/ccschem/articlecollection/minireviews

ALL OUR EDITORIALS IN ONE PLACE

Expanding chemistry through stories and reflections

In each monthly issue of *CCS Chemistry*, our editorials delve into great discoveries and amazing minds to provide a perspective of the research endeavor and the field of chemistry. Our editorials contain a short introduction to every article as well to give readers a quick snapshot of the research presented in the issue. Read all of our editorials for free at:
https://www.chinesechemsoc.org/journal/ccschem/articlecollection/editorial

CCS Chemistry

CCS Chemistry

RESEARCH ARTICLE

Received: Oct. 22, 2025 | Accepted: Dec. 11, 2025 | Published: Jan. 10, 2026

Giant Arenecage Enhancing Binding Affinity of Little Blue Box for Naphthalene Guests Through Host-in-Host Mechanism

Xiaoyun Dong[1], Congying Guo[1], Jiangshan Zhang[1], Qiao-Yan Qi[2], Hui Wang[1], Myongsoo Lee[1]*, Dan-Wei Zhang[1]* & Zhan-Ting Li[1,2]*

[1]*Department of Chemistry, Fudan University, Shanghai 200438,* [2]*State Key Laboratory of Organometallic Chemistry, Shanghai Institute of Organic Chemistry, Chinese Academy of Sciences, University of Chinese Academy of Sciences, Shanghai 200032*

**Corresponding authors: mslee@fudan.edu.cn; zhangdw@fudan.edu.cn; ztli@fudan.edu.cn*

Cite this: *CCS Chem.* **2026**, 8, 3971–3984
DOI: 10.31635/ccschem.025.202506895

Although a variety of Russian doll-styled non-intertwined box-in-box complexes have been reported, the utilization of this unique complexation pattern for the improvement of a specific property or function remains a challenging target. Herein, we report the construction of a box-in-cage assembly in aqueous solution from an anionic arenecage (ArCage) and the tetracationic little blue box (LBB) originally developed by Stoddart. Driven by both ion-pairing and donor–acceptor interactions, box-in-cage complex ArCage•LBB affords extremely high binding constant (K_a) of 6.35 × 10^7 M^{-1}. Stabilized by donor–acceptor interaction and hydrophobicity, LBB includes a variety of naphthalene derivative guests in water, with K_a values ranging from 9.80 × 10^4 M^{-1} to 2.81 × 10^7 M^{-1}. In the presence of ArCage, the K_a values for the complexation of LBB with naphthalenediols, naphthols, and naphthalene increases significantly, by up to 4.87 times, through exclusive encapsulation of the complexes by ArCage with the Russian doll mechanism. Enhancement of the hydrophobic cavity of LBB facilitated by ArCage has been proposed to account for the increased stability of the complexes formed between LBB and the naphthalene guests.

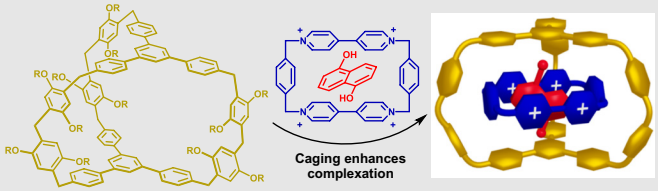

Keywords: molecular cage, host–guest chemistry, Russian doll, microenvironmental effect, inclusion enhancement

Introduction

The development of new strategies for enhancing host–guest complexation is of paramount importance in supramolecular chemistry.[1–11] Preorganization,[12,13] multivalency,[14,15] and structural adaptability[16–18] have been well-established as efficient strategies for the design of hosts that are able to exhibit high-affinity guest binding. Host–guest recognition between two macrocycles can lead to the formation of non-intertwined ring-in-ring superstructures,[19–25] while Russian doll-styled hierarchical host-in-host complexes have been used to construct higher-order mechanically interlocked Borromean rings[26–28] and spin crossover materials.[29] In principle, the outside host can provide a microenvironment that is different from the macroscopic medium to enable the

DOI: 10.31635/ccschem.025.202506895
Citation: *CCS Chem.* **2026**, 8, 3971–3984
Link to VoR: https://doi.org/10.31635/ccschem.025.202506895

inside host to achieve enhanced binding affinity for specific guests. Such microenvironment effect has been maximized by natural enzymes for the catalysis of various organic reactions that are vitally important for life.[30–32] Actually a number of large hosts have been demonstrated to include two or more guests to realize stable multicomponent complexation or improved reactivity.[33–43] However, for host-in-host systems, the utilization of the outside host-created microenvironment by the inside host for improving host–guest binding remains an interesting and challenging target.

Molecular cages feature three-dimensional spaces for efficient encapsulation of size-matching guests.[42,44–48] Water-soluble molecular cages can produce a hydrophobic cavity for including hydrophobic guests,[49–55] which may be further enhanced by additional ion-pair interactions. Compared to two-dimensional macrocycles, three-dimensional molecular cages possess superior structural confinement, which enhances the ability to precisely modulate the properties of encapsulated guest molecules. For example, a tetrahedral cage has been utilized to form an isolated water droplet in aqueous solution.[56] Giant cages are expected to encapsulate a large macrocyclic host to form host-in-host complexes in a Russian doll-like binding mechanism. It was envisioned that when the outside cage is able to produce a more closed hydrophobic space, the cage would be able to improve the stability of an included host–guest complex. The tetracationic cyclobis(paraquat-*p*-phenylene) cyclophane,[57] also known as little blue box (**LBB**), constitutes a modular electron-deficient receptor for the construction of a variety of host–guest complexes and mechanically interlocked supermolecules.[6,58–60] Although most investigations associated with this macrocycle have been performed in polar organic solvents with hexafluorophosphate as the counter ion, its tetrachloride salt is soluble in water and able to include catechols in water.[61] Herein, we report that water-soluble arenecage (**ArCage**) can produce a giant hydrophobic cavity to include **LBB** to form a highly stable host-in-host complex **ArCage•LBB**. We demonstrate that **ArCage** exhibits a pronounced microenvironment effect in both water and binary water/dimethyl sulfoxide (DMSO) medium, which enhances the affinity of the encapsulated **LBB** towards discrete naphthalenediols and naphthalenols via a Russian doll-like mechanism.

Experimental Methods

General methods

^{1}H and ^{13}C nuclear magnetic resonance (NMR) spectra were recorded with a Bruker AVANCE III HD 400 MHz spectrometer (101 MHz for ^{13}C NMR) in the indicated solvents at 25 °C. Chemical shifts were referenced to the signals of the residual nondeuterated solvent ($CDCl_3$: δ_H = 7.26 ppm, δ_C = 77.16 ppm; D_2O: δ_H = 4.79 ppm, DMSO-d_6: δ_H = 2.50 ppm, δ_C = 39.52 ppm, DMSO in D_2O: δ_C = 39.39 ppm). High-resolution mass spectrometric measurement was conducted on a Bruker McriOTOF11 (Billerica, Massachusetts, United States) or Waters G2-XS TOF spectrometer (Milford, Massachusetts, United States) coupled with an electrospray ionization (ESI) source, using a 0.5 mg/mL solution of sample in DMSO or deionized water. UV–vis absorption spectra were recorded on an Agilent Cary 100 UV–vis spectrophotometer (Cary, North Carolina, United States). Fluorescence spectra were recorded on a VARIAN CARY Eclipse Fluorescence Spectrophotometer (Cary, North Carolina, United States). UV–vis absorption and fluorescence emission spectra were measured at 25 °C using a 1 cm × 1 cm rectangular quartz cuvette on a spectrophotometer.

Determination of association constants

The binding constants was measured by fitting the UV–vis absorbance or fluorescence change to a 1:1 binding model using Origin 2025b. For direct host–guest titrations, the concentrated solution of a host was titrated into the solution of a guest. The equation of complexation between the host and the guest is expressed according to a 1:1 binding stoichiometry. The detailed methods are described in the Supporting Information.

Density functional theory calculations

Density functional theory (DFT) calculations were performed using DMol3 code in Materials Studio software 7.0 (Accelrys Inc, San Diego, California, United States). The exchange–correlation energy was calculated within the generalized gradient approximation using a Perdew–Burke–Ernzerhof (PBE) functional. As the PBE energy functional cannot describe the van der Waals dispersion interactions, a Grimme custom method for DFT-D correction was employed. The valence electron functions were expanded into a set of numerical atomic orbitals by a double numerical basis with polarization functions (DNP), all-electron core treatment. The convergence criteria of energy, displacement and force were 2×10^{-5} Ha, 5×10^{-3} Å, and 4×10^{-3} Ha/Å. The detailed procedures are described in Supporting Information.

Synthesis of compound 3

Compound **1** (4.55 g, 24.1 mmol) was dissolved in acetone (30 mL). To the solution, potassium carbonate (20.0 g, 144 mmol) was added. The suspended solution was stirred at 60 °C for 1 h, and then compound **2** (10.5 g, 57.8 mmol) was added. The mixture was stirred at 60 °C for 12 h and then cooled to room temperature. The solid was removed by filtration and washed with acetone (10 mL). The filtrate was concentrated with a rotavapor. The resulting residue was washed with water (2 mL × 3),

DOI: 10.31635/ccschem.025.202506895
Citation: *CCS Chem.* **2026**, 8, 3971–3984
Link to VoR: https://doi.org/10.31635/ccschem.025.202506895

dried in vacuo and then subjected to column chromatography on silica gel, using petroleum ether and ethyl acetate (10:1, v/v) as eluent, to give compound **3** as colorless oil (7.60 g, 81%). ^{1}H NMR ($CDCl_3$, δ): 7.09 (d, *J* = 2.79 Hz, 1H), 6.82 (d, *J* = 8.94 Hz, 1H), 6.77 (dd, *J* = 8.94, 2.80 Hz, 1H), 4.00 (t, *J* = 6.01 Hz, 2H), 3.94 (t, *J* = 6.09 Hz, 2H), 3.69 (s, 6H), 2.59 (t, *J* = 7.30 Hz, 2H), 2.51 (t, *J* = 7.26 Hz, 2H), 2.16–2.04 (m, 4H). ^{13}C NMR ($CDCl_3$, δ): 173.81, 173.69, 153.57, 149.74, 119.74, 115.55, 114.89, 114.48, 112.99, 68.97, 67.63, 51.77, 51.72, 30.58, 24.75, 24.72. High-resolution mass spectrometry (HRMS) (ESI) (*m/z*): $[M + Na]^+$ calcd for $C_{16}H_{21}BrO_6Na$, 411.0419; found, 411.0420.

Synthesis of compound 5

Compounds **3** (5.00 g, 12.8 mmol) and **4** (6.52 g, 25.7 mmol) were dissolved in 100 mL of toluene. To the solution were added potassium acetate (7.56 g, 77.1 mmol) and [1,1′-Bis(diphenylphosphino)-ferrocene] palladium(II) dichloride ($Pd(dppf)Cl_2$, 0.47 g, 5 mol %). The solution was stirred at 90 °C for 24 h and then cooled to room temperature. The precipitate formed was removed by filtration. The filtrate was concentrated with a rotavapor. The resulting residue was subjected to column chromatography on silica gel, using petroleum ether and ethyl acetate (5:1, v/v) as eluent to give compound **5** as light yellow oil. This compound was unstable at room temperature and used directly for the next step.

Synthesis of compound 7

Compounds **5** (4.47 g, 10.2 mmol) and **6**[62] (1.00 g, 1.71 mmol) were dissolved in 1,4-dioxane (40 mL). To the solution was added a solution of potassium carbonate (3.54 g, 25.6 mmol) in water. Catalyst $Pd(PPh_3)_4$ (20 mg, 5 mol %) was then added, and the mixture was stirred at 90 °C for 12 h. After cooling to room temperature, the solvent was removed with a rotavapor and the residue was treated with dichloromethane (100 mL). The solution was washed with washed (25 mL × 3), saline (25 mL), and dried over sodium sulfate. Upon removal of the solvent with a rotavapor, the resulting residue was subjected to column chromatography on silica gel, using petroleum ether and ethyl acetate (2:1, v/v) as eluent, to afford compound **7** as a white solid (1.30 g, 64%). ^{1}H NMR ($CDCl_3$, δ): 7.71 (d, *J* = 2.56 Hz, 3H), 7.58 (d, *J* = 7.68 Hz, 6H), 7.28 (d, *J* = 8.32 Hz, 6H), 6.80–6.65 (m, 9H), 4.01–3.88 (m, 18H), 3.67 (s, 9H), 3.62 (s, 9H), 2.50 (t, *J* = 7.35 Hz, 6H), 2.42 (t, *J* = 7.40 Hz, 6H), 2.03–2.09 (m, 12H). ^{13}C NMR ($CDCl_3$, δ): 173.86, 152.90, 150.99, 142.19, 140.37, 138.96, 130.94, 129.40, 127.33, 124.75, 117.77, 112.37, 112.28, 67.47, 67.29, 51.72, 51.68, 36.14, 30.71, 30.66, 24.91, 24.85. HRMS (ESI) (*m/z*): $[M + H]^+$ calcd for $C_{75}H_{85}O_{18}$, 1273.5736; found, 1273.5737.

Synthesis of compound 8

Compound **7** (0.45 g, 0.36 mmol) was dissolved in dichloromethane (45 mL). Polyoxymethylene (36 mg, 1.17 μmol) was then added. The reaction mixture was stirred at room temperature for 10 min, and then boron trifluoride diethyl etherate (3 mL) was added slowly. The mixture was stirred at 35 °C for 1 h and then poured onto ice (30 g). The organic phase was separated, washed with water (15 mL × 3), saline (15 mL), dried over sodium sulfate, and concentrated with a rotavapor. The resulting residue was subjected to column chromatography on silica gel, using petroleum ether and ethyl acetate (1:1, v/v) as eluent, to give compound **8** as yellow solid (0.12 g, 30%). ^{1}H NMR ($CDCl_3$ δ): 7.49 (s, 6H), 7.38 (d, *J* = 8.12 Hz, 12H), 7.20 (d, *J* = 7.91 Hz, 12H), 6.77 (s, 6H), 6.64 (s, 6H), 3.92–3.83 (m, 42H), 3.68 (s, 18H), 3.58 (s, 18H), 2.51 (t, *J* = 7.44 Hz, 12H), 2.43 (t, *J* = 7.39 Hz, 12H), 2.41–2.33 (m, 24H). ^{13}C NMR ($CDCl_3$, δ): 173.72, 173.64, 150.37, 150.20, 141.94, 140.53, 138.82, 129.11, 128.52, 127.83, 127.03, 124.53, 114.97, 114.39, 67.57, 67.33, 51.63, 51.52, 36.29, 30.78, 30.63, 25.08, 24.91. HRMS (ESI) (*m/z*): $[M + 2Na]^{2+}$ calcd for $C_{153}H_{168}O_{36}Na_2$, 1314.0573; found, 1314.0571.

Synthesis of ArCage

Compound **8** (0.10 g, 0.039 mmol) was dispersed in methanol (10 mL). To the solution was added aqueous solution of sodium hydroxide (40%, 10 mL). The mixture was stirred at 80 °C for 12 h, then cooled to room temperature, and then concentration with a rotavapor to about 10 mL. Aqueous hydrochloric acid solution was added dropwise to pH = 3. The solid formed was filtrated off and then dispersed in water (3 mL). To the solution was added aqueous solution of sodium hydroxide (2 M), dropwise, to pH = 9. The solution was concentrated with a rotavapor to about 1 mL and then loaded into a dialysis bag (molecular weight cutting-off: 1000 Da). The bag was put into stirred water (1 L) for dialysis for 12 h. The solution was then concentrated with a rotavapor, washed with acetone (0.5 mL × 3), and dried in vacuo to afford **ArCage** as a white solid (67 mg, 64%). ^{1}H NMR (CD_3OD, δ): 7.49 (s, 6H), 7.41 (d, *J* = 7.84 Hz, 12H), 7.22 (d, *J* = 7.96 Hz, 12H), 6.92 (s, 6H), 6.72 (s, 6H), 3.91–3.84 (m, 42H), 2.41–2.33 (m, 24H), 2.12–2.00 (m, 24H). ^{13}C NMR (CD_3OD, δ): 180.45, 180.31, 150.67, 150.42, 142.06, 140.75, 138.61, 128.84, 128.70, 127.86, 126.62, 123.92, 115.02, 114.44, 68.45, 68.32, 48.10, 47.89, 47.67, 47.45, 35.59, 33.78, 26.35, 26.25. HRMS (matrix assisted laser desorption ionization-time of flight (MALDI-TOF)) was recorded for the corresponding carboxylic aci. HRMS (MALDI-Tof) (*m/z*): $[M + Na]^+$ calcd for $C_{141}H_{144}O_{36}Na$, 2435.934; found, 2435.967.

Synthesis of compound NP-a

Compound **NP-c** (2.00 g, 12.5 mmol) was added to a stirred solution of sodium hydroxide (10%) in water

DOI: 10.31635/ccschem.025.202506895
Citation: *CCS Chem.* **2026**, 8, 3971–3984
Link to VoR: https://doi.org/10.31635/ccschem.025.202506895

(16 mL). Then a solution of 1,3-propanesultone (3.80 g, 31.2 mmol) in dioxane (24 mL) was added under stirring. The solution was stirred at room temperature for 12 h. The precipitate formed was collected by filtration and then recrystallized from dioxane and water (1:1) to afford compound NP-a as a white solid (3.03 g, 54%). ^{1}H NMR (DMSO-d_6, δ): 7.71 (d, J = 8.37 Hz, 2H), 7.39 (t, J = 8.03 Hz, 2H), 6.96 (d, J = 7.66 Hz, 2H), 4.23 (t, J = 6.37 Hz, 4H), 2.70 (t, J = 7.08 Hz, 4H), 2.19–2.12 (m, 4H). ^{13}C NMR (D_2O, δ): 126.21, 126.01, 114.14, 106.98, 48.12, 24.38. HRMS (ESI) (m/z): [M + H]$^+$ calcd for $C_{16}H_{19}O_8Na_2S_2$, 449.0317; found, 449.0317.

Synthesis of compound NP-b

This compound was synthesized as a white solid according to a reported method.[63] ^{1}H NMR ($CDCl_3$, δ): 7.85 (d, J = 8.43 Hz, 2H), 7.34 (t, J = 8.06 Hz, 2H), 6.84 (d, J = 7.63 Hz, 2H), 4.30 (t, J = 4.93 Hz, 4H), 3.99 (t, J = 4.85 Hz, 4H), 3.81 (dd, J = 5.96, 3.52 Hz, 4H), 3.72–3.61 (m, 24H), 3.60–3.54 (m, 4H). ^{13}C NMR ($CDCl_3$, δ): 154.35, 126.79, 125.09, 114.63, 105.70, 72.53, 71.01, 70.68, 70.59, 70.29, 69.83, 67.93, 61.74. HRMS (ESI) (m/z): [M + H]$^+$ calcd for $C_{30}H_{49}O_{12}$, 601.3224; found, 601.3206.

Results and Discussion

Scheme 1a provides the structures of the compounds used in this study. The preparation of **ArCage** is shown in Scheme 1b. Thus, compound **1** was first reacted with **2** in acetone in the presence of potassium carbonate to afford compound **3** in 81% yield. Palladium-catalyzed coupling of compounds **3** and **4** in toluene afforded compound **5** in 54% yield. Further palladium-catalyzed coupling of **5** and tribromide **6**[54] in dioxane and water produced compound **7** in 64% yield. This intermediate was then treated with paraformaldehyde in dichloromethane in the presence of boron trifluoride to afford neutral molecular cage **8** in 30% yield, which followed the method reported for the preparation of the prototypical neutral molecular cage that bears twelve methoxy groups.[55] Finally, compound **8** was hydrolyzed with sodium hydroxide in methanol and water to give rise to **ArCage** in 64% yield. The solubility of **ArCage** in water was determined to be 107 mg/mL.

The crystal structure of the prototypical neutral molecular cage that bears 12 methoxy groups showed that the two 1,3,5-triphenylbenzene units have a spatial separation of 8.4 Å,[56] which is larger than the width of **LBB** (averagely 7.0 Å).[57] We thus first evaluated the binding affinity of **ArCage** to **LBB** using ^{1}H NMR spectroscopy by gradually adding **ArCage** to the solution of **LBB** (0.8 mM) in D_2O. Adding 0.5 equiv of **ArCage** caused the four signals of **LBB** to vanish completely (Figure 1a,b and Supporting Information Figure S1), which indicated that the free and **ArCage**-included **LBB** molecules underwent slow exchange on the ^{1}H NMR timescale. Upon further addition of 0.5 equiv of **ArCage**, **LBB** displayed a new set of NMR signals, wherein the H-a–d signals (Scheme 1a) exhibited significant shifting from 9.13 to 7.98 ppm, 8.30 to 7.73 ppm, 7.65 to 8.18 & 7.68 ppm, 5.87 to 3.96 ppm, respectively. The H-a,b,d signals shifted upfield remarkably, supporting that these protons were located in the cavity of **ArCage** and thus underwent important shielding. It is noteworthy that H-c exhibited two isolated signals, which were downfield compared with that of the free H-c, suggesting that two benzene rings of **LBB** were orientated at different positions outside the cavity of **ArCage**, thus underwent deshielding effect of the cavity, and could not exchange rapidly. The fact that the exchange of the free and included **LBB** molecules in the presence of **ArCage** was slow on the ^{1}H NMR timescale provided the first evidence supporting the high stability of the complex. ^{1}H nuclear Overhauser effect spectroscopy of the 1:1 mixture of **ArCage** and **LBB** in D_2O showed intermolecular connection between the H-a–c signals of **LBB** and the signals of the aromatic units of **ArCage** (Supporting Information Figure S2), further confirming the inclusion of **LBB** in the cavity of **ArCage** (Figure 2a). The binding constant (K_a) of complex **ArCage•LBB** in water was then measured. For this aim, we first performed direct UV–vis titration of rhodamine B (RhB) with **ArCage** (Supporting Information Figure S3). Fitting the change in UV–vis absorbance at 555 nm to a standard 1:1 binding model, which was confirmed by Job plot (Supporting Information Figure S3), allowed the determination of K_a for complex **ArCage•**RhB ($(9.98 \pm 0.35) \times 10^6$ M^{-1}, Table 1). We then performed competitive binding assays by treating solutions containing fixed concentrations of **ArCage** and **RhB** with increasing concentrations of **LBB** and measuring the UV–vis response (Figure 3a). By fitting the change of the UV–vis absorbance at 575 nm (Figure 3a) to a competitive binding model and using the known K_a value of complex **ArCage•RhB** as input, we determine the K_a value of complex **ArCage•LBB** [$(6.35 \pm 0.22) \times 10^7$ M^{-1}, Table 1].

We then investigated the binding affinity of **LBB** for discrete **NP-a–h** as electron-rich guests. Extensive studies have illustrated that naphthalene derivatives form 1:1 donor–acceptor complexes with **LBB**.[57,58] Gradually adding **LBB** to the solution of dianionic **NP-a** in D_2O caused continuous weakening of the H-2–4 signals, which were at 7.11 (d), 7.52 (dd), and 7.94 (d) ppm, respectively, of **NP-a** in the ^{1}H NMR spectrum (Supporting Information Figure S4).[64] When the amount of **LBB** increased to higher than 0.5 equiv, these three signals vanished completely, and a new set of signals at 2.46, 6.18, and 6.46 ppm, respectively, appeared (Figure 1a and Supporting Information Figure S4), which were assigned by comparing with those of related compounds.[56,57] This observation clearly showed that two compounds formed

DOI: 10.31635/ccschem.025.202506895
Citation: *CCS Chem.* **2026**, 8, 3971–3984
Link to VoR: https://doi.org/10.31635/ccschem.025.202506895

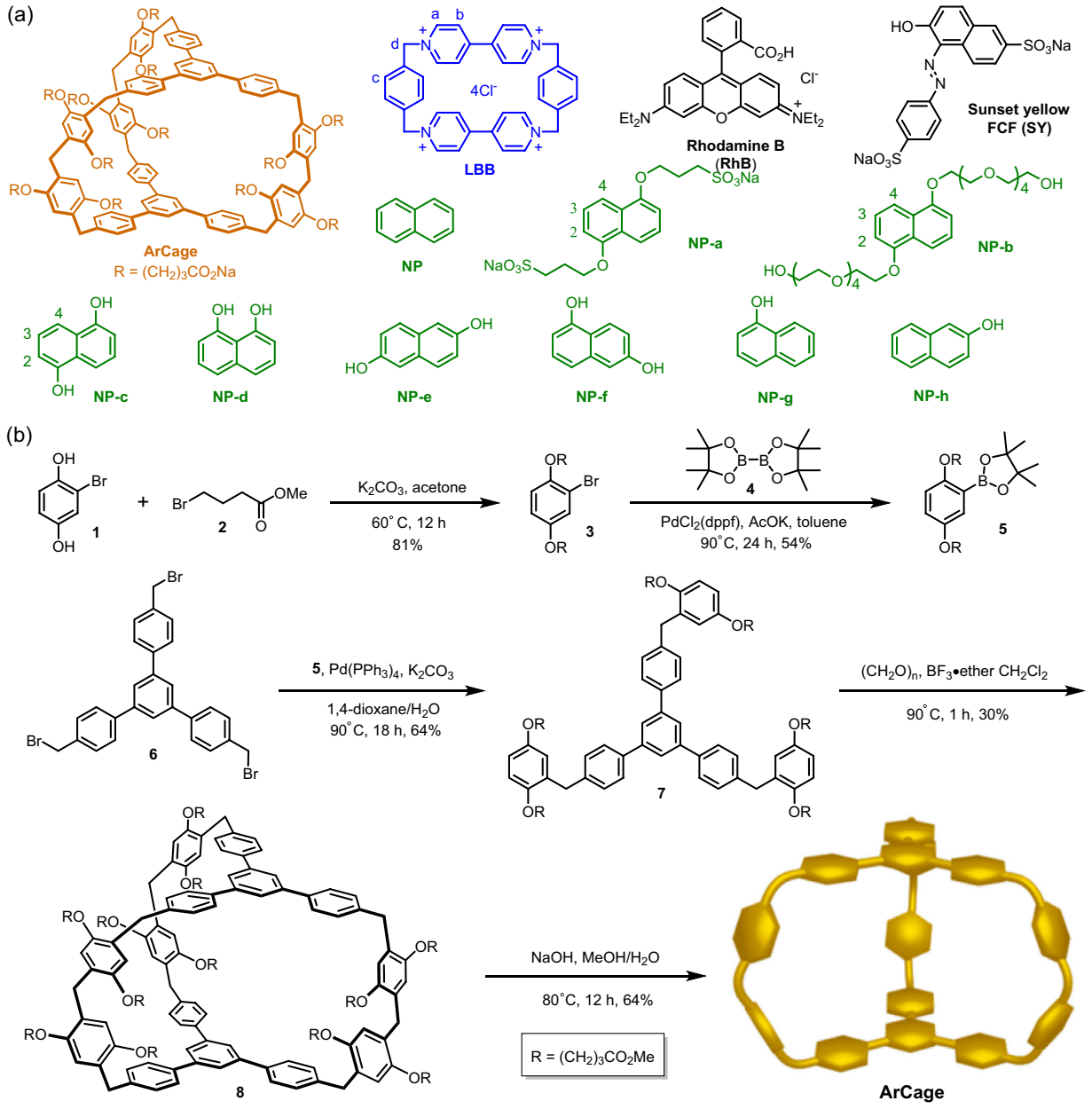

Scheme 1 | *(a) The structures of compounds used for this study. (b) The synthetic route for* ***ArCage****.*

stable 1:1 donor–acceptor complex **LBB•NP-a** (Figure 2a) and the exchange between the free and **LBB**-included **NP-a** molecules was slow on the ^{1}H NMR timescale. To determine the K_a of the complex, we first performed a direct UV–vis titration of sunset yellow food color forming (SY) with **LBB** (Supporting Information Figure S5), which gave rise to K_a of (1.27 ± 0.16) × 10^6 M^{-1}, Table 1) for complex **LBB•**SY. We further performed competitive binding assays using UV–vis absorption spectroscopy by treating solutions containing fixed concentrations of **LBB** and SY with increasing concentrations of **NP-a** (Figure 3b). By fitting the change of the UV–vis absorbance at 479 nm to a competitive binding model and using the known K_a value of complex **LBB•**SY as input, we determine the K_a value of complex **LBB•NP-a** ((2.81 ± 0.24) × 10^7 M^{-1}, Table 1).

We further evaluated the binding affinity of **LBB** for discrete neutral naphthalene guests. ^{1}H NMR in D_2O showed that **NP-b** and **LBB** also formed a stable 1:1 complex (Figure 2b), which exhibited a new set of signals in the upfield area for the aromatic protons of the complexed **NP-b** (Supporting Information Figure S6), as observed for the 1:1 mixture of **NP-a** and **LBB**. Compound **NP-b** exhibited strong fluorescence centered around 329 nm, which was strongly quenched by **LBB**. We thus performed direct fluorescence titration of **NP-b** with **LBB**

DOI: 10.31635/ccschem.025.202506895
Citation: *CCS Chem.* **2026**, 8, 3971–3984
Link to VoR: https://doi.org/10.31635/ccschem.025.202506895

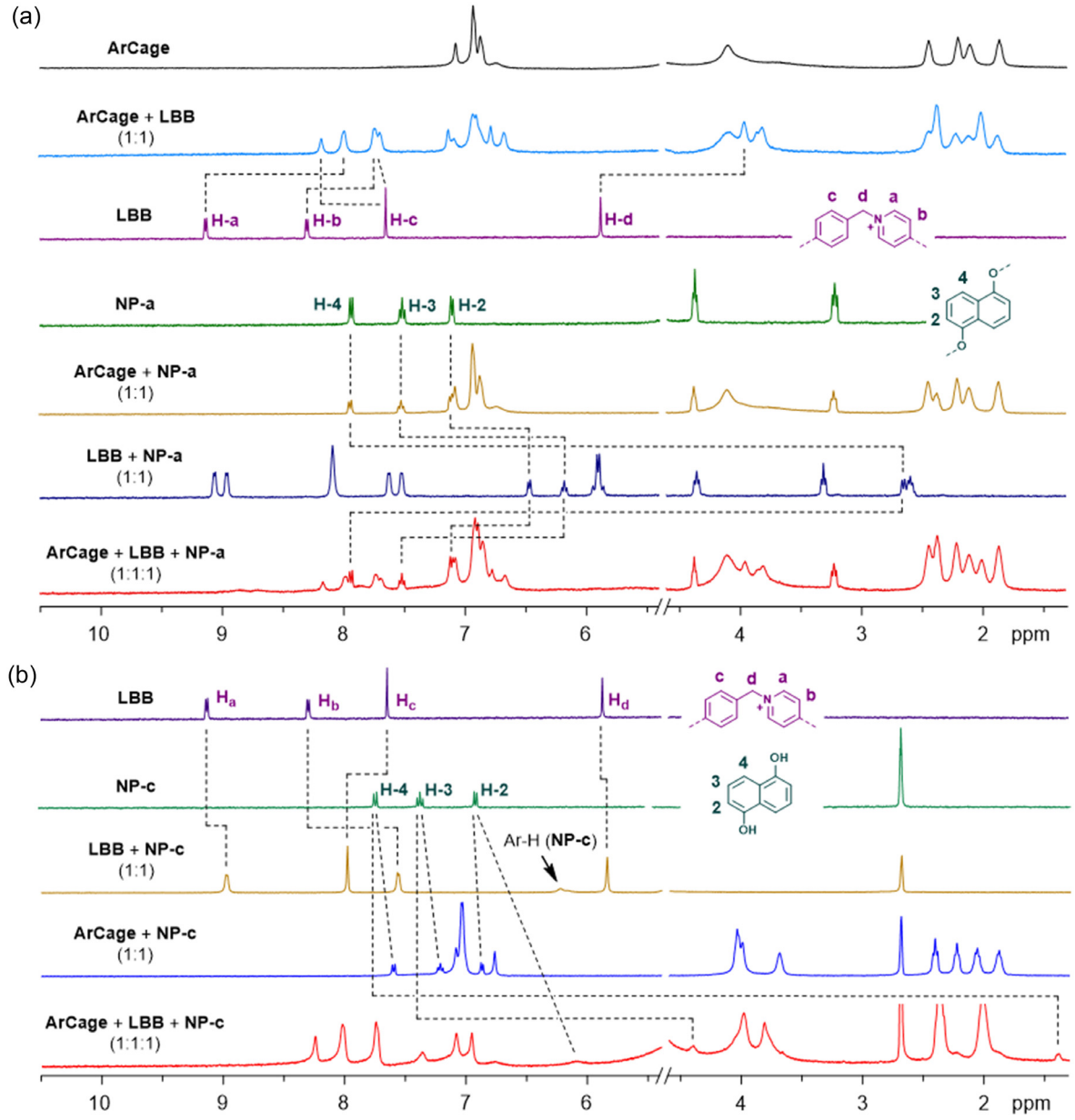

Figure 1 | *^{1}H NMR spectra (400 MHz at 25 °C): (a)* ***ArCage***, ***LBB***, ***NP-a****, and their di- and tri-component mixtures in D_2O. (b)* ***LBB*** *in D_2O and* ***NP-c*** *and di- and tri-component mixtures in D_2O and DMSO-d_6 (95%:5%, v/v) ([**ArCage**] = [**LBB**] = [**NB-a**] = [**NP-c**] = 0.8 mM).*

(Supporting Information Figure S7). Fitting of the change of the fluorescence of **NP-b** at 329 nm to a 1:1 binding model led to the determination of K_a for complex **LBB•NP-b** [(4.39 ± 0.22) × 10^5 M^{-1}, Table 1]. In a similar manner, we determined the K_a values of the complexes formed between **LBB** and naphthalenediols **NP-c**∼**f** as well as naphthols, that is, **NP-g** and **NP-h** (Figure 3c and Supporting Information Figures S8–S13). Among all the naphthalene guests, **NP-a** exhibited the highest binding affinity, which indicated that, in addition to donor–acceptor interactions between its naphthalene unit and the 4,4′-bipyridinium units of **LBB**, there existed important ion-pair electrostatic attraction between its two sulfonate groups and the pyridinium units of **LBB**.

The naphthalene unit is hydrophobic and thus may be included into the hydrophobic cavity of **ArCage** in water. We thus further evaluated the binding affinity of **ArCage** for all the naphthalene derivatives. Addition of up to 1.2 equiv of **ArCage** to a solution of **NP-a** in D_2O did not cause observable shifting of the signals corresponding to the aromatic protons of **NP-a** in the ^{1}H NMR spectra (Figure 1a and Supporting Information Figure S14). This result indicated that no significant binding occurred between the two anionic compounds reasonably due to

DOI: 10.31635/ccschem.025.202506895
Citation: *CCS Chem.* **2026**, 8, 3971–3984
Link to VoR: https://doi.org/10.31635/ccschem.025.202506895

Table 1 | *Binding Constants (K_a) Determined by Direct and Competitive UV–vis and Fluorescence Assays for Complexes Formed by **ArCage**, **LBB**, and Naphthalene Derivatives at 25 °C*[a]

	ArCage K_{a1}	**LBB** K_{a2}	**ArCage⊂LBB** K_{a3}	K_{a2}/K_{a3}	
			($\times10^5$ M^{-1}, in H_2O)		
RhB	99.8 ± 3.5				
LBB	635 ± 22[b]				
SY			12.7 ± 1.6		
NP-a	no		281 ± 24[c]	no	
NP-b	4.17 ± 0.20		4.39 ± 0.22	2.96 ± 0.15	0.67
NP-c	1.16 ± 0.20		8.46 ± 0.20	21.4 ± 0.70	2.53
NP-d			0.98 ± 0.06	4.76 ± 0.40	4.87
NP-e			1.40 ± 0.15	3.11 ± 0.08	2.22
NP-f			4.01 ± 0.10	5.14 ± 0.28	1.28
NP-g			3.27 ± 0.10	9.29 ± 0.09	2.84
NP-h			1.72 ± 0.03	3.50 ± 0.30	2.03
			($\times10^5$ M^{-1}, in H_2O/DMSO (95%/5%, v/v))		
NP-b			4.56 ± 0.21	3.43 ± 0.08	0.75
NP-c			9.76 ± 0.62	20.2 ± 0.60	2.07
NP-d			1.70 ± 0.24	3.50 ± 0.18	2.06
NP-e			1.58 ± 0.13	2.40 ± 0.06	1.52
NP-f			3.44 ± 0.10	5.40 ± 0.45	1.57
NP-g			2.53 ± 0.17	5.84 ± 0.25	2.31
NP-h			0.97 ± 0.06	2.52 ± 0.19	2.59
			[$\times10^5$ M^{-1}, in H_2O/DMSO (90%/10%, v/v)]		
NP			2.71 ± 0.08	4.78 ± 0.15	1.76
NP-b			3.04 ± 0.18	2.00 ± 0.10	0.66
NP-c			6.75 ± 0.14	11.3 ± 1.30	1.67
NP-d			1.07 ± 0.05	1.80 ± 0.13	1.68
NP-e			1.15 ± 0.02	1.89 ± 0.20	1.64
NP-f			2.17 ± 0.12	2.80 ± 0.06	1.29
NP-g			1.66 ± 0.03	2.60 ± 0.17	1.57
NP-h			0.74 ± 0.05	1.53 ± 0.06	2.06

[a] All data are the average of three repetitive determinations.
[b] Using UV–vis competitive assays with RhB as dye.
[c] Using UV–vis competitive assays with SY as dye.

electrostatic repulsion of their anionic ions. Adding **ArCage** to the solution of neutral, but water-soluble **NP-b** in D_2O led to rapid decrease of the resolution of the signals of **NP-b** in the ^{1}H NMR spectra (Supporting Information Figure S15). Moreover, the resonance signals for all aromatic protons in **NP-b** exhibited consistent upfield shifting. With the addition of 1.0 equiv of **ArCage**, the signals shifted from 7.10, 7.53, and 7.93 ppm to 5.46, 6.44, and 6.83 ppm, respectively, supporting that its naphthalene unit was encapsulated by the cavity of **ArCage** driven by hydrophobicity and thereby experienced important shielding effect from the triphenylbenzene units of **ArCage**. Adding **ArCage** to the solution of **NP-b** in water also resulted in the quenching of the fluorescence of **NP-b** (Supporting Information Figure S16). Fitting of the change of the fluorescence at 333 nm to a 1:1 binding model allowed for the determination of K_a for complex **ArCage•NP-b** [(4.17 ± 0.20) × 10^5 M^{-1}, Table 1]. Using the same method, the K_a of complex **ArCage•NP-c** was determined to be (1.16 ± 0.20) × 10^5 M^{-1} (Table 1, Figure 3d). Owing to fluorescence spectral overlap, the K_a values of the complexes between **ArCage** and **NP-d ~ h** could not be determined by the same method.

The influence of **ArCage** on the binding affinity of **LBB** for the naphthalene guests was then studied. The complexation of **LBB** with **NP-a** led to an almost complete quenching of the fluorescence of **NP-a** in water (Supporting Information Figure S17). Adding **ArCage** to their 1:1 solution could result in the recovery of the fluorescence (Supporting Information Figure S18), indicating that **NP-a** was expelled from the cavity of **LBB**. ^{1}H NMR spectra further confirmed that adding **ArCage** to a 1:1 mixture of **LBB** and **NP-a** in D_2O prompted the release of the naphthalene unit of **NP-a** from the cavity of **LBB** (Figure 1a and

DOI: 10.31635/ccschem.025.202506895
Citation: *CCS Chem.* **2026**, 8, 3971–3984
Link to VoR: https://doi.org/10.31635/ccschem.025.202506895

Supporting Information Figure S19). This was evidenced by the fact that, in the three-component solution, **NP-a** existed primarily in a free, uncomplexed state, while **ArCage** and **LBB** formed a 1:1 complex. These observations confirmed that **ArCage** included **LBB** and extruded **NP-a** from the cavity of **LBB**. Given the rigidity of **LBB**, the encapsulation of **ArCage** for **LBB** should not suppress the donor–acceptor interaction between **LBB** and the naphthalene unit of **NP-a**. Thus, it is reasonable to propose that the electrostatic repulsion between the carboxylate groups of **ArCage** and the sulfonate groups of **NP-a** was stronger than the donor–acceptor interaction, thereby expelling the naphthalene unit of **NP-a** from the cavity of **LBB**.

The K_a value of complex **ArCage•LBB** was substantially higher than that of **ArCage•NP-b**, suggesting that in the 1:1:1 solution of **ArCage**, **LBB**, and **NP-b**, complex **ArCage•LBB** was formed preferentially. Adding **LBB** to the 1:1 solution of **ArCage** and **NP-b** in water caused remarkable quenching of the fluorescence of both compounds (Supporting Information Figure S20). Adding the mixture of **ArCage** and **LBB** (1:1) to the solution of **NP-b** in water also caused the quenching of the fluorescence of **NP-b** (Supporting Information Figure S7). Both observations supported the formation of three-component complex **ArCage⊂LBB•NP-b** in the Russian doll-styled manner (Figure 2b). Upon addition of **ArCage** to the 1:1 mixture of **LBB** and **NP-b** in D_2O, the ^{1}H NMR signals corresponding to H-a–c of **LBB**, which originally appeared at 8.97, 8.05, and 7.50 ppm, respectively, exhibited further upfield shifting (Supporting Information Figure S21). When 1.0 equiv of **ArCage** was added to the 1:1 mixture of **LBB** and **NP-b** in D_2O, the H-2 and H-3 signals of **NP-b** in the ^{1}H NMR spectrum shifted upfield from 6.16 and 6.44 ppm to 5.84 and 6.07 ppm, respectively. This observation further supports the formation of a three-component complex, in which the naphthalene ring of **NP-b** experienced dual shielding effects from the bipyridinium units of **LBB** and the triphenylbenzene units of **ArCage**. By fitting the change in the emission of **NP-b** at 344 nm (Supporting Information Figure S7) to a standard 1:1 binding model, we could determine the K_a for complex **ArCage⊂LBB•NP-b** to be (2.96 ± 0.15) × 10^5 M^{-1} (Table 1). The value was discernibly lower than that observed in the absence of **ArCage**, suggesting that **ArCage** imposed little spatial repulsion for the inclusion of **LBB** for **NP-b** (Figure 2b). Molecular modeling showed that, for the lowest-energy structure of the ternary complex **ArCage⊂LBB⊂NP-b** (Figure 2b), the two glycol chains extruded from the cavity of **ArCage** (Figure 4a). Given the rigidity of both **LBB** and **ArCage** in the ternary complex, it is reasonable to propose that the flexibility of the two hydrophilic glycol chains of **NP-b** was restricted by both of them, which disfavored the inclusion of **LBB** for **NP-b**.

The binding affinity (K_{a3}) of **LBB** for **NP-c–h** in the presence of **ArCage** was then investigated in water by adding **LBB** and **ArCage** (1:1) to the aqueous solutions of **NP-c ~ h** and recording the quenching of the fluorescence of the **naphthalene** guests (Figure 3e,f and Supporting Information Figures S7–S13). By fitting the change in emission at a specific wavelength to a 1:1 binding model, we determined the K_{a3} values for **LBB•NP-c–h** complexes in the six ternary complexes **ArCage⊂LBB•NP-c–h** (Figure 2c, Table 1). These values were 2.53, 4.87, 2.22, 1.28, 2.84, and 2.03 times that of the same complex in the absence of **ArCage**. All the values were substantially lower than that of complex **ArCage•LBB**, which meant that, when the binding of **LBB** for the naphthalene guests occurred, **LBB** existed mainly in the form of complex **ArCage•LBB**. For all the titrations, the two compounds were added at the same molar concentrations to the solution of the naphthalene guests. Thus, these K_{a3} values may be considered as apparent ones. All the goodness-of-fit (R^2) values of the nonlinear regressions were ≥0.99, which confirmed the feasibility of the treatment. Adding **NP-c** (0.3–2.5 equiv) to the solution of **LBB** and **ArCage** (1:1) in D_2O and DMSO-d_6 (95%/5% v/v) did not cause the appearance of the signals of the free **NP-c** in the ^{1}H NMR spectra (Supporting Information Figure S22). Instead, the spectra only gave rise to the signals of the encapsulated species. Moreover, their chemical shifts were nearly unchanged with the increase of **NP-c**. The addition of DMSO-d_6 was used to improve the solubility of **NP-c**, which has limited solubility in pure water. Thus, the exchange of the encapsulated **NP-c** and the unencapsulated **P-c** was slow on the NMR timescale, even though the unencapsulated species did not afford observable signals.

The addition of DMSO to the solution diminished the enhancing effect of **ArCage** on the stability of the complexes. When DMSO concentration was increased from 5 to 10 vol % (Table 1, Supporting Information Figures S23–S36 and Tables S1–S7), the enhancement effect remained observable, but was less pronounced. Therefore, we attributed the enhancement effect in pure water to the increased hydrophobicity of **ArCage**. In the binary media, **ArCage** should cause more generalized solvophobic effect, which, together with the donor–acceptor interaction formed between naphthalene guests and **LBB**, accounted for the less pronounced, but observable stability enhancement. ^{1}H NMR analysis in D_2O and DMSO-d_6 (95%/5% v/v) further demonstrated that the addition of **ArCage** to the **LBB•NP-c** complex resulted in a significant upfield shifting of one signal of **NP-c**, even though another two signals were not observed (Scheme 1a and Figure 1b). The assignment of the signals of **NP-c** of the tricomponent complex was assigned by comparing with those of the reported related compound.[64,65]

The addition of 5% DMSO-d_6 enabled good solubility for **NP-c** for the ^{1}H NMR experiments. The signals of **NP-c** were assigned by comparing with those of **NP-a**. In the presence of 1.0 equiv of **LBB**, the H-3 signal underwent 0.80 ppm of upfield shifting. With the addition of 1.0 equiv of **ArCage**, the signal further suffered another 0.15 ppm of

DOI: 10.31635/ccschem.025.202506895
Citation: *CCS Chem.* **2026**, 8, 3971–3984
Link to VoR: https://doi.org/10.31635/ccschem.025.202506895

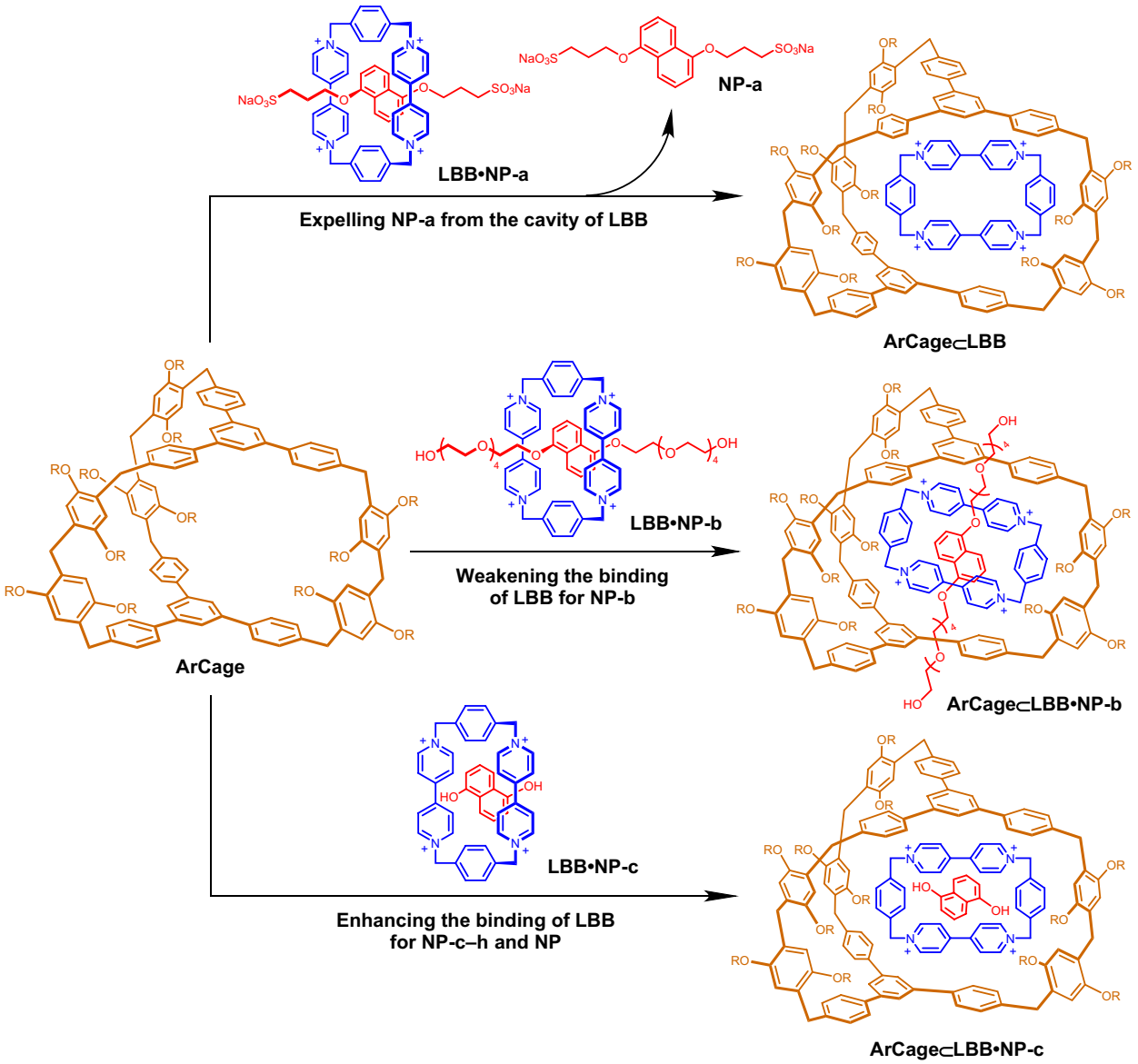

Figure 2 | *Schematic representations of three different effects of the encapsulation of **ArCage** for **LBB** on the latter's inclusion for naphthalene guests in water: (a) extruding **NP-a**, (b) weakening **NP-b** inclusion, and (c) enhancing **NP-c–h** and **NP** inclusion.*

upfield shifting. Molecular modeling for the ternary complex of **NP-c** revealed that complex **LBB•NP-c** adopted two distinct binding orientations within the **ArCage** cavity. In one case, the bipyridinium units of **LBB** formed stacking interactions with the two triphenylbenzene units of **ArCage** (Figure 4b). In another one, the bipyridinium units are stacked loosely with two diphenylmethane linkers of **ArCage** (Figure 4c). In both cases, **NP-c** was largely enveloped by the backbones of **LBB**, **ArCage**, as well as the appendant side chains of **ArCage**. This suggests that **ArCage** and **LBB** collaboratively form a more enclosed and solvaphobic cavity, which exhibits enhanced inclusion capability toward smaller guest molecules such as naphthalene diols and mono-naphthols.

The binding constants of complex **LBB•NP-c** in water and the two binary solvents were all substantially higher than that (up to 1.5 × 10^3 M^{-1}) of the complex in acetonitrile.[66,67] For 1,5-dioxynaphthalene derivatives that bear two $(OCH_2CH_2)_nOH$ (n = 1, 2, 3), the binding constant of their complexes with **LBB** in water was also significantly higher than that obtained in acetonitrile, which has been attributed to the hydrophobicity in water.[66] Naphthalene diols and their ether derivatives are typical electron-rich aromatic compounds.[66] We thus further investigated the binding of **LBB** for less electron-rich naphthalene (**NP**) in the absence and presence of **ArCage**. Since **NP** was insoluble in water, we conducted fluorescence titration experiments in binary water and

DOI: 10.31635/ccschem.025.202506895
Citation: *CCS Chem.* **2026**, 8, 3971–3984
Link to VoR: https://doi.org/10.31635/ccschem.025.202506895

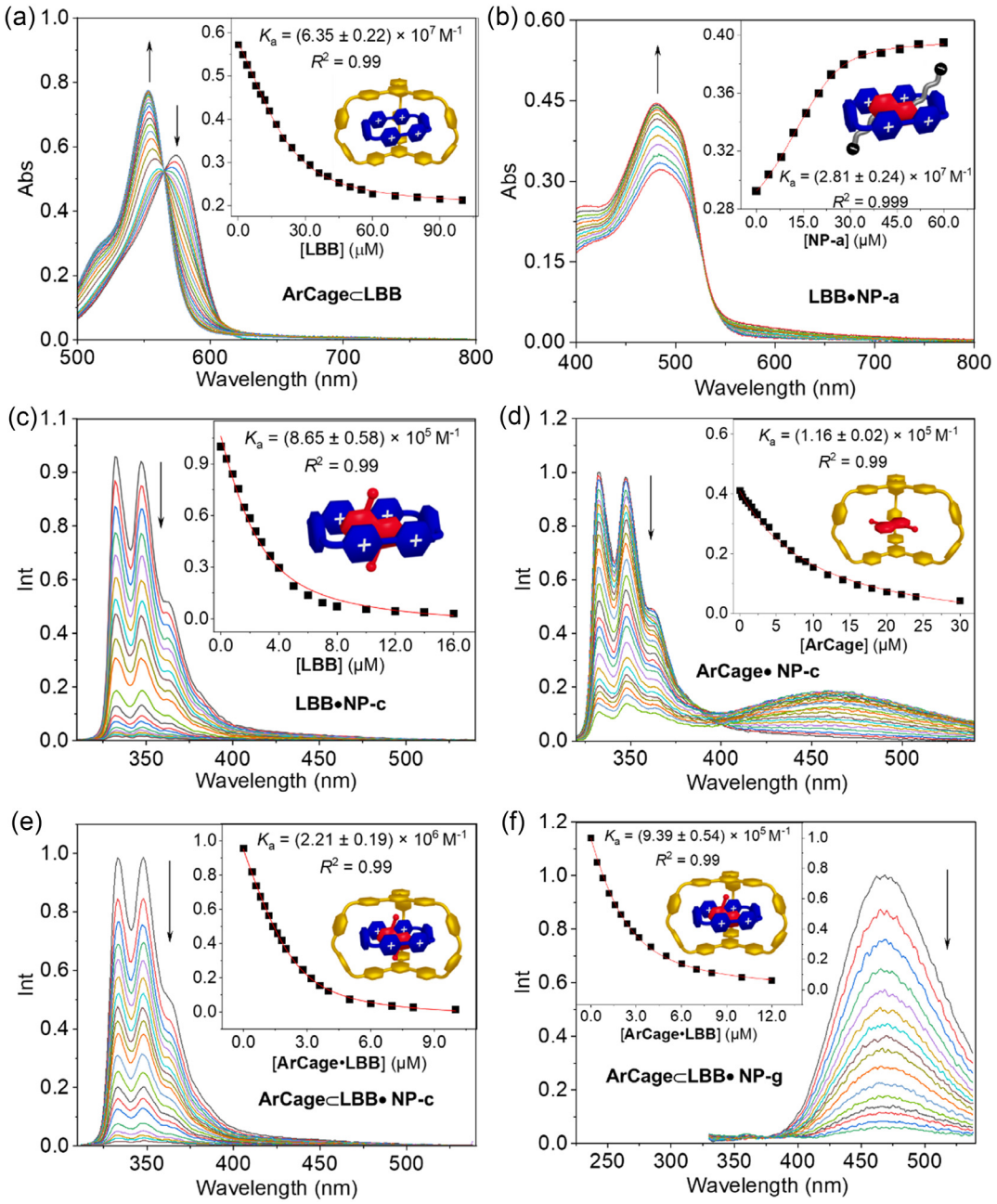

Figure 3 | *UV–vis and fluorescence titration assays in water: (a) spectra of the solution of RhB (10 μM) and* ***ArCage*** *(10 μM) with the addition of* ***LBB*** *(0–100 μM). Inset: plot of the absorbance of RhB at 575 nm vs [****LBB****]. (b) UV–vis spectra of the solution of SY (20 μM) and* ***LBB*** *(20 μM) with the addition of* ***NP-a*** *(0–60 μM). Inset: plot of the absorbance of SY at 505 nm vs [****NP-a****]. (c) Fluorescence spectra of* ***NP-c*** *(2 μM, λ_{ex} = 290 nm) with the addition of* ***LBB*** *(0-20 μM). Inset: plot of fluorescence intensity of* ***NP-c*** *at 336 nm vs [****LBB****]. (d) Fluorescence spectra of* ***NP-c*** *(2 μM, λ_{ex} = 290 nm) with the addition of* ***ArCage*** *(0-30 μM). Inset: plot of fluorescence intensity of* ***NP-c*** *at 336 nm vs [****ArCage****]. (e) Fluorescence spectra of (e)* ***NP-c*** *(2 μM, λ_{ex} = 290 nm) and (f)* ***NP-g*** *(2 μM, λ_{ex} = 310 nm) with the addition of* ***LBB*** *(0-11 μM) and* ***ArCage*** *(1:1) (0-12 μM). Inset: plot of fluorescence intensity of (e)* ***NP-c*** *at 344 nm and (f)* ***NP-g*** *at 456 nm vs [****LBB****] = [****ArCage****]. Figures c,e,f represent one of three repetitive titration results.*

DMSO (90%/10%, v/v) (Table 1 and Supporting Information Table S8 and Figure S37), which revealed that K_a of complex **LBB•NP** in the presence of **ArCage** was 1.76 times that of the complex in the absence of the cage. Moreover, in both cases, the K_a value was comparable with the corresponding one of different naphthalene diols, but higher than that of the complexes formed between **LBB** and **NP-c** or its ether derivatives in acetonitrile.[66,67] These results also supported that solvophobic effect might be the main driving force for all the above

DOI: 10.31635/ccschem.025.202506895
Citation: *CCS Chem.* **2026**, 8, 3971–3984
Link to VoR: https://doi.org/10.31635/ccschem.025.202506895

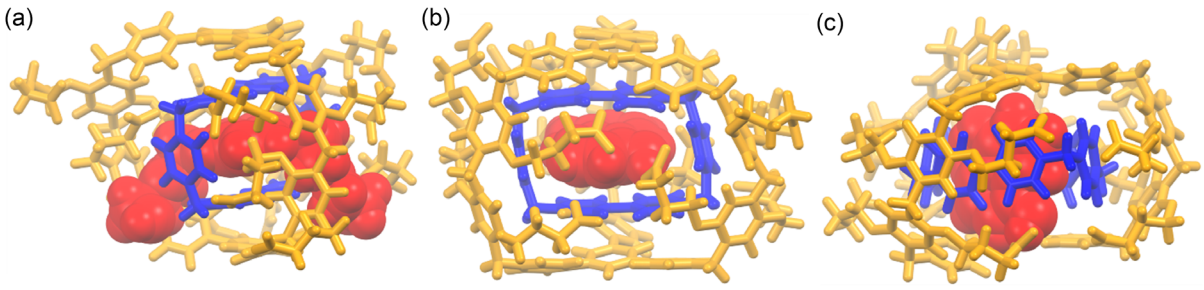

Figure 4 | *DFT-optimized low-energy structures of ternary complexes (a)* ***ArCage⊂LBB•NP-b*** *and (b, c)* ***ArCage⊂LBB•NP-c*** *(The bipyridinium units of* ***LBB*** *are roughly stacked with the triphenylbenzene units or the diphenylmethane linkers of* ***ArCage****). For simplification, the* $(OCH_2CH_2)_5OH$ *groups of* ***NP-b*** *were replaced with the shorter* $(OCH_2CH_2)_2OH$ *groups.*

complexes in water or the binary solvents, which was further enhanced by **ArCage**.

The above results demonstrated that the presence of **ArCage** led to three different influences on the binding of **LBB** for naphthalene guests. For dianionic naphthalene guest **NP-a**, electrostatic repulsion between its sulfonate groups and the carboxylate groups of **ArCage** was large enough to surpass the donor–acceptor and hydrophobic interactions formed between it and **LBB**, leading to complete suppression of their complexation. For neutral **NP-b** that bears two long $(OCH_2CH_2)_5OH$ chains, the two chains imposed spatial repulsion to weaken the binding of **LBB** for it due to the encapsulation of **LBB** by **ArCage**. For smaller guests **NP** and **NP-c–h**, similar spatial repulsion was very weak or did not exist. The encapsulation of **ArCage** for **LBB** increased the closure and hydrophobicity of its cavity. As a result, **LBB** could realize enhanced binding affinity for these smaller guests in both water and the binary solvents through the cage-in-cage mechanism.

Conclusion

We have prepared a highly water-soluble dodecaanionic molecular cage that incorporates a tetracationic **LBB** in water with K_a value of 6.35×10^7 M^{-1}. The anionic molecular cage produces a giant hydrophobic cavity to include blue box driven by donor–acceptor and ion-pair electrostatic interactions. This inclusion increases the hydrophobicity of the cavity of **LBB** and reduces the exposure of the included naphthalene guests to the highly polar macroenvironment. As a result, its binding affinity for naphthalenediols and naphthols can be enhanced significantly. The result illustrates the potential of the Russian doll inclusion pattern to create a microenvironment capable of enhanced encapsulation efficiency for specific guest molecules. The molecular cage has a D_{3h}-symmetric backbone. In principle, a tritopic cationic cage can be designed to feature a more enclosed and size-matched cavity, which may facilitate unprecedented levels of guest inclusion and enhanced dynamic behavior.

Supporting Information

Supporting Information is available and includes compound synthesis and characterization (Figures S38–S49), theoretical computational detail, photophysical properties.

Conflict of Interest

The authors declare no conflict of interest.

Funding Information

This work was financially supported by the National Natural Science Foundation of China (grant nos. 22271059 and 22531011) for financial support.

References

1. Kyba, E. P.; Helgeson, R. C.; Madan, K.; Gokel, G. W.; Tarnowski, T. L.; Moore, S. S.; Cram, D. J. Host–Guest Complexation. 1. Concept and Illustration. *J. Am. Chem. Soc.* **1977**, *99*, 2564–2571.
2. Liu, P.; Fang, F.; Wang, H.; Khashab, N. M. Smart Materials Based on Synthetic Host Molecules: The Role of Host–Guest Chemistry in the Fabrication and Application. *Angew. Chem. Int. Ed.* **2023**, *62*, e202218706.
3. Sarkar, S.; Ballester, P.; Spektor, M.; Kataev, E. A. Micromolar Affinity and Higher: Synthetic Host–Guest Complexes with High Stabilities. *Angew. Chem. Int. Ed.* **2023**, *62*, e202214705.
4. Han, X.-N.; Han, Y.; Chen, C.-F. Recent Advances in the Synthesis and Applications of Macrocyclic Arenes. *Chem. Soc. Rev.* **2023**, *52*, 3265–3298.

DOI: 10.31635/ccschem.025.202506895
Citation: *CCS Chem.* **2026**, 8, 3971–3984
Link to VoR: https://doi.org/10.31635/ccschem.025.202506895

5. Ma, Y.-L.; Yan, S.; Xu, X.-J.; Cao, H.; Wang, R. Synthetic Host–Guest Pairs as Novel Bioorthogonal Tools for Pre-targeting. *Chin. Chem. Lett.* **2024**, *35*, 108645.
6. Feng, Y.; Zhao, X.; Appleton Daniel, A.; Han, H.; Young Ryan, M.; Liu, W.; Lee Christopher, K.; Li, W.; Liu, B.-T.; Wu, Y.; Tang, C.; Chen Aspen, X. Y.; Stern Charlotte, L.; Kim Dong, J.; Wasielewski Michael, R.; Qiu, Y.; Stoddart, J. F. Chalcogen-oviologen Enhanced Host–Guest Recognition. *CCS Chem.* **2024**, *6*, 2679–2691.
7. Li, G.; Lewis Reece, W.; Eelkema, R. Out-of-Equilibrium Assembly Based on Host–Guest Interactions. *CCS Chem.* **2023**, *6*, 27–40.
8. Hong, Q.-Y.; Huang, B.; Wu, M.-X.; Xu, L.; Zhao, X.-L.; Shi, X.; Yang, H.-B. Redox-Active Dihydrophenazine-Based Macrocycle: Synthesis, Conformation-Adaptive Behavior and Host–Guest Complexation with Tetracyanoquinodimethane. *Chin. J. Chem.* **2024**, *42*, 1895–1900.
9. Chen, F.-Y.; Fu, R.; Gong, Z.; Li, C.; Guo, D.-S.; Cai, K. Ultrahigh-Affinity Molecular Recognition in Water and Biomedical Applications. *Angew. Chem. Int. Ed.* **2025**, *64*, e202500916.
10. Yang, J.; Lou, X.-Y.; Dai, D.; Shi, J.; Yang, Y.-W. Desymmetrized Pillar[8]arenes: High-Yield Synthesis, Functionalization, and Host–Guest Chemistry. *Chin. Chem. Lett.* **2025**, *36*, 109818.
11. Zhou, W.; He, Q. Redefining Host–Guest Chemistry Through Amphoteric Chalcogen and Halogen Bonding. *Sci. Chin. Chem.* **2025**, *68*, 3909–3911.
12. Van Eerden, J.; Grootenhuis, P. D. J.; Dijkstra, P. J.; Van Staveren, C. J.; Harkema, S.; Reinhoudt, D. N. Effect of Preorganization of Macrocyclic Hosts on the Complexation of Neutral Molecules. *J. Org. Chem.* **1986**, *51*, 3918–3920.
13. Yu, H.-M.; Yu, X.-Y.; Chen, Y. Preorganized Cationic Pillararene as Efficient Carriers for Intracellularly Delivering Native Proteins. *Chin. Chem. Lett.* **2023**, *34*, 108037.
14. Huskens, J.; Mulder, A.; Auletta, T.; Nijhuis, C. A.; Ludden, M. J. W.; Reinhoudt, D. N. A Model for Describing the Thermodynamics of Multivalent Host–Guest Interactions at Interfaces. *J. Am. Chem. Soc.* **2004**, *126*, 6784–6797.
15. Badjić, J. D.; Cantrill, S. J.; Grubbs, R. H.; Guidry, E. N.; Orenes, R.; Stoddart, J. F. The Exclusivity of Multivalency in Dynamic Covalent Processes. *Angew. Chem. Int. Ed.* **2004**, *43*, 3273–3278.
16. Banerjee, R.; Bhandari, P.; Hickey, N.; Mukherjee, P. S. Guest-Shape-Directed Structural Switching Between Two Isomers of a Pd_6 Host and Its Structural Adaptability for Selective Photodimerization. *J. Am. Chem. Soc.* **2025**, *147*, 23049–23059.
17. Hollstein, S.; von Delius, M. The Dynamic Chemistry of Orthoesters and Trialkoxysilanes: Making Supramolecular Hosts Adaptive, Fluxional, and Degradable. *Acc. Chem. Res.* **2024**, *57*, 602–612.
18. von Krbek, L. K. S.; Achazi, A. J.; Schoder, S.; Gaedke, M.; Biberger, T.; Paulus, B.; Schalley, C. A. The Delicate Balance of Preorganisation and Adaptability in Multiply Bonded Host–Guest Complexes. *Chem. Eur. J.* **2017**, *23*, 2877–2883.
19. Liu, D.; Li, K.; Chen, M.; Zhang, T.; Li, Z.; Yin, J.-F.; He, L.; Wang, J.; Yin, P.; Chan, Y.-T.; Wang, P. Russian-Doll-Like Molecular Cubes. *J. Am. Chem. Soc.* **2021**, *143*, 2537–2544.
20. Xia, Y.; Jiang, Y.; Ni, X.-L.; Wang, Q.; Wang, D. A Macrocycle-Based "Russian Doll": The Smallest Cucurbit[4]uril in Cucurbit[10]uril. *Chin. Chem. Lett.* **2024**, *35*, 109782.
21. Cai, K.; Lipke, M. C.; Liu, Z.; Nelson, J.; Cheng, T.; Shi, Y.; Cheng, C.; Shen, D.; Han, J.-M.; Vemuri, S.; Feng, Y.; Stern, C. L.; Goddard, W. A.; Wasielewski, M. R.; Stoddart, J. F. Molecular Russian Dolls. *Nat. Commun.* **2018**, *9*, 5275.
22. Lei, Z.; Polen, S.; Hadad, C. M.; RajanBabu, T. V.; Badjić, J. D. Russian Nesting Doll Complexes of Molecular Baskets and Zinc Containing TPA Ligands. *J. Am. Chem. Soc.* **2016**, *138*, 8253–8258.
23. Gong, W.; Yang, X.; Zavalij, P. Y.; Isaacs, L.; Zhao, Z.; Liu, S. From Packed "Sandwich" to "Russian Doll": Assembly by Charge-Transfer Interactions in Cucurbit[10]uril. *Chem. Eur. J.* **2016**, *22*, 17612–17618.
24. Day, A. I.; Blanch, R. J.; Arnold, A. P.; Lorenzo, S.; Lewis, G. R.; Dance, I. A Cucurbituril-Based Gyroscane: A New Supramolecular Form. *Angew. Chem. Int. Ed.* **2002**, *41*, 275–277.
25. Zhang, Y.; Liu, Y.; Wu, Y.; Ge, C.; Li, B.; Wei, Y.; Qian, Y.; Li, Q.; Huang, F.; Li, H. A Tetracationic Cyclophane. *CCS Chem.* **2025**, *7*, 50–58.
26. Huang, S.-L.; Lin, Y.-J.; Li, Z.-H.; Jin, G.-X. Self-Assembly of Molecular Borromean Rings from Bimetallic Coordination Rectangles. *Angew. Chem. Int. Ed.* **2014**, *53*, 11218–11222.
27. Kim, T.; Singh, N.; Oh, J.; Kim, E.-H.; Jung, J.; Kim, H.; Chi, K.-W. Selective Synthesis of Molecular Borromean Rings: Engineering of Supramolecular Topology via Coordination-Driven Self-Assembly. *J. Am. Chem. Soc.* **2016**, *138*, 8368–8371.
28. Gao, X.; Liu, D.; Zhang, H.-N.; Jin, G.-X. Coordination-Driven Self-Assembly of a Molecular 8_{18} Knot and Molecular Borromean Rings. *Sci. Chin. Chem.* **2024**, *67*, 3652–3656.
29. Guionneau, P.; Marchivie, M.; Chastanet, G. Multiscale Approach of Spin Crossover Materials: A Concept Mixing Russian Dolls and Domino Effects. *Chem. Eur. J.* **2021**, *27*, 1483–1486.
30. Hosseini, M. W.; Lehn, J. M.; Maggiora, L.; Mertes, K. B.; Mertes, M. P. Supramolecular Catalysis in the Hydrolysis of ATP Facilitated by Macrocyclic Polyamines: Mechanistic Studies. *J. Am. Chem. Soc.* **1987**, *109*, 537–544.
31. Bilal, M.; Cui, J.; Iqbal, H. M. N. Tailoring Enzyme Microenvironment: State-of-the-Art Strategy to Fulfill the Quest for Efficient Bio-Catalysis. *Int. J. Biol. Macromol.* **2019**, *130*, 186–196.
32. James, C. C.; de Bruin, B.; Reek, J. N. H. Transition Metal Catalysis in Living Cells: Progress, Challenges, and Novel Supramolecular Solutions. *Angew. Chem. Int. Ed.* **2023**, *62*, e202306645.
33. Murase, T.; Nishijima, Y.; Fujita, M. Cage-Catalyzed Knoevenagel Condensation Under Neutral Conditions in Water. *J. Am. Chem. Soc.* **2012**, *134*, 162–164.
34. Sun, D.; Huang, X.; Han, X.; Liu, S. Precise Control of Noncovalent Dimerization via Cucurbit[n]uril-Based Host–Guest Complexation. *Org. Lett.* **2025**, *27*, 3249–3253.

DOI: 10.31635/ccschem.025.202506895
Citation: *CCS Chem.* **2026**, 8, 3971–3984
Link to VoR: https://doi.org/10.31635/ccschem.025.202506895

35. Liu, S.; Zavalij, P. Y.; Isaacs, L. Cucurbit[10]uril. *J. Am. Chem. Soc.* **2005**, *127*, 16798–16799.
36. Liu, S.; Shukla, A. D.; Gadde, S.; Wagner, B. D.; Kaifer, A. E.; Isaacs, L. Ternary Complexes Comprising Cucurbit[10]uril, Porphyrins, and Guests. *Angew. Chem. Int. Ed.* **2008**, *47*, 2657–2660.
37. Zhou, Y.; Yang, J.; Jie, K. Macrocyclic Arene-Based Metal–Organic Cages. *Coord. Chem. Rev.* **2025**, *539*, 216726.
38. Luo, N.; Ao, Y.-F.; Wang, D.-X.; Wang, Q.-Q. Exploiting Anion–π Interactions for Efficient and Selective Catalysis with Chiral Molecular Cages. *Angew. Chem. Int. Ed.* **2021**, *60*, 20650–20655.
39. Sun, H.; Wang, X.-Y.; Wang, X.-D.; Ao, Y.-F.; Wang, D.-X.; Wang, Q.-Q. Selective Alkane Desaturation Catalyzed by Molecular Cage Copper Complexes Under Mild Conditions. *CCS Chem.* **2024**, *6*, 1876–1884.
40. Chen, L.; Tan, M.; Jin, J.; Zhang, Z.; Huang, F.; Li, S.; Li, Y. Synthesis and Application of Chiral Organic Imine Molecular Cages. *Chin. J. Org. Chem.* **2024**, *44*, 2617–2639.
41. Chai, Q.; Duan, L.; Ma, Y.; Hou, T.; Tu, T. Recent Advances in the Synthesis and Application of *N*-Heterocyclic Carbene-Based Molecular Cages. *Sci. Chin. Chem.* **2024**, *67*, 1510–1523.
42. Mao, C.; He, Y.; Wang, X.; Cai, Y.; Hu, X. Synthesis and Molecular Recognition Characteristics of a Tetrapodal Benzene Cage. *Chin. Chem. Lett.* **2024**, *35*, 109362.
43. Yang, T.; Shen, Y.; Qu, H.; Li, B.; Sun, Y.; Wu, G. Quaternary 2:2 Complexes as Kinetic Intermediates: Unveiling an Overlooked Pathway in Cucurbit[8]uril-Mediated Assembly. *CCS Chem.* **2025**, *7*, 2978–2986.
44. Takezawa, H.; Tabuchi, R.; Sunohara, H.; Fujita, M. Confinement of Water-Soluble Cationic Substrates in a Cationic Molecular Cage by Capping the Portals with Tripodal Anions. *J. Am. Chem. Soc.* **2020**, *142*, 17919–17922.
45. Montà-González, G.; Sancenón, F.; Martínez-Máñez, R.; Martí-Centelles, V. Purely Covalent Molecular Cages and Containers for Guest Encapsulation. *Chem. Rev.* **2022**, *122*, 13636–13708.
46. Wang, Q.-Q. Anion Recognition-Directed Supramolecular Catalysis with Functional Macrocycles and Molecular Cages. *Acc. Chem. Res.* **2024**, *57*, 3227–3240.
47. Acharyya, K.; Mukherjee, P. S. Organic Imine Cages: Molecular Marriage and Applications. *Angew. Chem. Int. Ed.* **2019**, *58*, 8640–8653.
48. Zhang, Y.; Zhou, J.; Luo, K.; Zhou, W.; Wang, F.; Li, J.; He, Q. Ferritin-Inspired Encapsulation and Stabilization of Gold Nanoclusters for High-Performance Photothermal Conversion. *Angew. Chem. Int. Ed.* **2025**, *64*, e202500058.
49. Percástegui, E. G.; Ronson, T. K.; Nitschke, J. R. Design and Applications of Water-Soluble Coordination Cages. *Chem. Rev.* **2020**, *120*, 13480–13544.
50. Fang, S.; Li, E.; Zhu, D.; Wu, G.; Zhang, Q.; Lin, C.; Huang, F.; Li, H. A Water-Soluble Naphthalenediimide-Containing Hexacationic Cage. *Chem. Commun.* **2021**, *57*, 6074–6077.
51. Duan, Y.; Wang, J.; Cheng, L.; Duan, H.; Tian, P.; Zhang, Y.; Cao, L. A Fluorescent, Chirality-Responsive, and Water-Soluble Cage as a Multifunctional Molecular Container for Drug Delivery. *Org. Biomol. Chem.* **2022**, *20*, 3998–4005.
52. Maji, S.; Samanta, J.; Natarajan, R. Water-Soluble Triazolium Covalent Cages for ATP Sensing. *Chem. Eur. J.* **2024**, *30*, e202303596.
53. Liyana Gunawardana, V. W.; Ward, C.; Wang, H.; Holbrook, J. H.; Sekera, E. R.; Cui, H.; Hummon, A. B.; Badjić, J. D. Crystalline Nanoparticles of Water-Soluble Covalent Basket Cages (CBCs) for Encapsulation of Anticancer Drugs. *Angew. Chem. Int. Ed.* **2023**, *62*, e202306722.
54. Zhuang, S.-Y.; Wu, G.; Sun, J.-D.; Zhang, J.; Xing, J.; Wu, Y.; Wang, H.; Li, Z.-T.; Zhang, D.-W. Water-Soluble Hexakis-Imidazolium Cages: Synthesis and Selective Binding of Sodium Urate. *Org. Chem. Front.* **2024**, *11*, 414–421.
55. Zhong, Y.-M.; Xia, Z.-J.; Hu, Y.-H.; Zhou, L.-P.; Cai, L.-X.; Sun, Q.-F. Effective Separation of Phenanthrene from Isomeric Anthracene Using a Water-Soluble Macrocycle-Based Cage. *Chin. Chem. Lett.* **2025**, *36*, 110164.
56. Sebastiani, F.; Bender, T. A.; Pezzotti, S.; Li, W.-L.; Schwaab, G.; Bergman, R. G.; Raymond, K. N.; Toste, F. D.; Head-Gordon, T.; Havenith, M. An Isolated Water Droplet in the Aqueous Solution of a Supramolecular Tetrahedral Cage. *PNAS* **2020**, *117*, 32954–32961.
57. Odell, B.; Reddington, M. V.; Slawin, A. M. Z.; Spencer, N.; Stoddart, J. F.; Williams, D. J. Cyclobis(paraquat-p-phenylene). A Tetracationic Multipurpose Receptor. *Angew. Chem. Int. Ed.* **1988**, *27*, 1547–1550.
58. Chen, X.-Y.; Chen, H.; Stoddart, J. F. The Story of the Little Blue Box: A Tribute to Siegfried Hünig. *Angew. Chem. Int. Ed.* **2023**, *62*, e202211387.
59. Neira, I.; Blanco-Gómez, A.; Quintela, J. M.; García, M. D.; Peinador, C. Dissecting the "Blue Box": Self-Assembly Strategies for the Construction of Multipurpose Polycationic Cyclophanes. *Acc. Chem. Res.* **2020**, *53*, 2336–2346.
60. Dale, E. J.; Vermeulen, N. A.; Juríček, M.; Barnes, J. C.; Young, R. M.; Wasielewski, M. R.; Stoddart, J. F. Supramolecular Explorations: Exhibiting the Extent of Extended Cationic Cyclophanes. *Acc. Chem. Res.* **2016**, *49*, 262–273.
61. Bernardo, A. R.; Stoddart, J. F.; Kaifer, A. E. Cyclobis (paraquat-p-phenylene) as a Synthetic Receptor for Electron-Rich Aromatic Compounds: Electrochemical and Spectroscopic Studies of Neurotransmitter Binding. *J. Am. Chem. Soc.* **1992**, *114*, 10624–10631.
62. Zhang, J.-N.; Li, H.; Zhou, W.; Yu, S.-L.; Qu, D.-H.; Tian, H. Fluorescence Modulation in Tribranched Switchable [4] Rotaxanes. *Chem. Eur. J.* **2013**, *19*, 17192–17200.
63. Sagara, Y.; Seki, A.; Kim, Y.; Tamaoki, N. Linearly Polarized Photoluminescence from an Asymmetric Cyclophane Showing Thermo- and Mechanoresponsive Luminescence. *J. Mater. Chem. C* **2018**, *6*, 8453–8459.
64. Li, H.; Cheng, C.; McGonigal, P. R.; Fahrenbach, A. C.; Frasconi, M.; Liu, W.-G.; Zhu, Z.; Zhao, Y.; Ke, C.; Lei, J.; Young, R. M.; Dyar, S. M.; Co, D. T.; Yang, Y.-W.; Botros, Y. Y.; Goddard III, W. A.; Wasielewski, M. R.; Astumian, R. D.; Stoddart, J. F. Relative Unidirectional Translation in an Artificial Molecular Assembly Fueled by Light. *J. Am. Chem. Soc.* **2013**, *135*, 18609–18620.

DOI: 10.31635/ccschem.025.202506895
Citation: *CCS Chem.* **2026**, 8, 3971–3984
Link to VoR: https://doi.org/10.31635/ccschem.025.202506895

65. López-Vidal, E. M.; Prokofjevs, A.; Gibbs-Hall, I. C.; Dale, E. J.; Quintela, J. M.; Peinador, C. Studies Towards the Synthesis of Pd(II)-Containing [2] and [3] Catenanes in Aqueous Media. *Dalton T.* **2018**, *47*, 2492–2496.
66. Venturi, M.; Dumas, S.; Balzani, V.; Cao, J.; Stoddart, J. F. Threading/Dethreading Processes in Pseudorotaxanes. A Thermodynamic and Kinetic Study. *New J. Chem.* **2004**, *28*, 1032–1037.
67. Williams, D. J.; Ashton, P. R.; Ballardini, R.; Balzani, V.; Credi, A.; Gandolfi, M. T.; Menzer, S.; Perez-Garcia, L.; Prodi, L. Molecular Meccano. 4. The Self-Assembly of [2]Catenanes Incorporating Photoactive.pi.-Extended Systems. *J. Am. Chem. Soc.* **1995**, *117*, 11171–11197.

DOI: 10.31635/ccschem.025.202506895
Citation: *CCS Chem.* **2026**, 8, 3971–3984
Link to VoR: https://doi.org/10.31635/ccschem.025.202506895